Periodic structures of magnetic garnet particles for strong Faraday rotation enhancement

A. Christofi* and N. Stefanou
University of Athens, Department of Solid State Physics, Panepistimioupolis, GR-157 84 Athens, Greece

N. Papanikolaou
Institute of Nanoscience and Nanotechnology, NCSR "Demokritos," GR-153 10 Athens, Greece
(Received 23 January 2014; revised manuscript received 2 June 2014; published 12 June 2014)

We show that a relatively sparse photonic crystal of high-permittivity magnetic garnet particles can induce a giant Faraday rotation of light transmitted through a finite slab of it. The underlying mechanism resides in wave propagation through collective Bloch modes, which are strongly localized in the particles.

DOI: 10.1103/PhysRevB.89.214410 PACS number(s): 42.70.Qs, 78.20.Ls, 42.25.Bs

I. INTRODUCTION

Composite structures comprising magnetic materials exhibit intriguing optical and magneto-optical (MO) properties, including spectral nonreciprocity and increased nonlinear response, circular dichroism, Faraday and Kerr effects. For example, large Faraday and Kerr effects, as a result of the strong field localization in the magneto-optically active material, have been demonstrated in one-dimensional structures, such as a magnetic thin film sandwiched between dielectric Bragg mirrors [1] and magnetic/dielectric multilayer films at the edges of their photonic band gap [2,3]. A modification of the MO spectral response, especially prominent near the photonic band edges, was also observed in three-dimensional self-assembled inverse opal structures infiltrated with magnetic nickel nanoparticles [4]. Moreover, it has been shown that resonant Kerr effect can be obtained with subwavelength nanowire gratings made of MO dielectric materials, for a given polarization of the incident light, by tuning the incidence angle and grating parameters to operate near the resonant reflectance condition for the orthogonal polarization state [5]. On the other hand, suitable combinations of magnetic materials with noble metals at different geometries, e.g., multilayers [6–10], nanosandwiches [11–13], core-shell particles [14–17], and noble-metal nanoparticles optically coupled with magnetic films or particles [18–20], though suffering from absorptive losses, can also enhance the MO effects due to the strong electromagnetic (EM) fields that arise from the surface plasmon excitation in the noble metal.

In the present work, we seek to combine the field enhancement induced by localized Mie resonances of high-permittivity nanoparticles and the strong MO response of low-loss garnet materials in the same structural unit of a three-dimensional photonic crystal and show that this crystal can induce a huge Faraday rotation of light transmitted through a finite slab of it, which largely exceeds that obtained in other designs. Our results are obtained by means of rigorous, full electrodynamic numerical calculations using the layer-multiple-scattering method [21,22] that we recently extended to photonic crystals of gyrotropic spheres [23].

At visible and infrared frequencies, the gyrotropic response of magnetic materials is rather weak and can be described by a relative magnetic permeability $\mu_g = 1$ and a relative electric permittivity tensor of the form

$$\overleftrightarrow{\epsilon_g} = \epsilon \begin{pmatrix} 1 & -ig & 0 \\ ig & 1 & 0 \\ 0 & 0 & 1 \end{pmatrix}, \tag{1}$$

if the magnetization points in the z direction. In the present work, we shall assume $\epsilon = 6.25$ and $g = 0.01$, values which are achievable with magnetic garnets [24–26].

II. A PHOTONIC CRYSTAL OF UNMAGNETIZED GARNET SPHERES

The optical response of a single unmagnetized garnet sphere [$g = 0$ in Eq. (1)], of radius S, is characterized by strong and spectrally separated magnetic (H) and electric (E) multipole (2^l-pole, $l = 1,2,3,\ldots$) Mie resonances, with increased field intensity in the region of the sphere, as shown in Fig. 1. Interestingly, though the first electric dipole resonance is smeared out, the fundamental magnetic dipole resonance is well defined and resolved, which is in agreement with the results of García-Etxarri *et al.* [27].

If such spheres are assembled into a sparse periodic structure, narrow photonic bands of collective Bloch states are formed from the resonant modes of the individual particles, weakly interacting between them. The wave field associated with these states maintains a strongly localized character in the region of the spheres. In addition to the above narrow bands, there are of course extended bands of propagating modes in the homogeneous host medium. Anticrossing interaction between narrow and extended bands of the same symmetry gives rise to the formation of frequency gaps and hybridized bands that have strong admixture of the localized modes in their flat parts, near the boundaries and the center of the first Brillouin zone. Such a photonic band diagram, along the [001] direction of a simple cubic crystal of unmagnetized garnet spheres with a radius to lattice constant ratio $S/a = 0.3$, in air, is shown in Fig. 2. Along the given crystallographic direction, the bands have the symmetry of the irreducible representations of the C_{4v} point group [28], and thus they are either nondegenerate or doubly degenerate. It is worth noting that only the doubly degenerate bands can be excited by light incident normally on a finite (001) slab of the crystal. The nondegenerate bands are optically inactive, because they do not have the proper symmetry, and in a finite slab of the crystal correspond to bound states of the

*aristi@ims.demokritos.gr

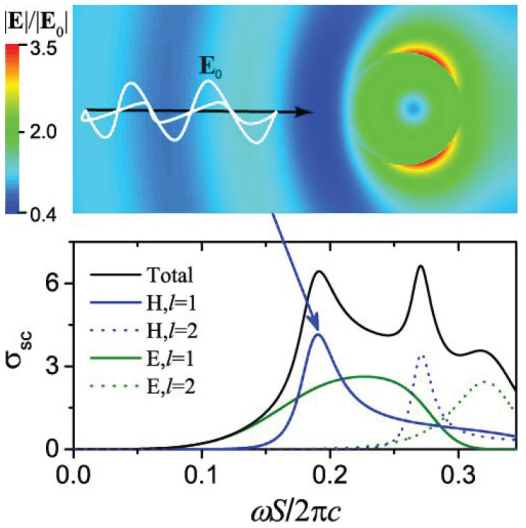

FIG. 1. (Color online) The scattering cross section spectrum, normalized to the geometrical cross section, and its multipole decomposition, associated with a plane EM wave incident on the single unmagnetized garnet sphere, of radius S, in air. Above the cross section diagram we display the relative (with respect to the incident plane wave) electric-field amplitude distribution corresponding to the fundamental magnetic-dipole resonant mode.

EM field that decrease exponentially outside the slab on either side of it.

III. FARADAY ROTATION INDUCED BY A CRYSTAL OF MAGNETIC GARNET SPHERES

If the garnet spheres are magnetized along the z direction, i.e., in the Faraday geometry [$g = 0.01$ in Eq. (1)], the symmetry is lowered and each doubly degenerate band of the dispersion diagram of Fig. 2 splits into two nondegenerate bands. These bands have the symmetry of left- and right-circularly polarized (LCP and RCP, respectively) propagating waves, and thus can be excited by appropriately polarized light, incident normally on a finite (001) slab of the crystal. In Fig. 3, next to the dispersion diagram of the photonic crystal of magnetized garnet spheres along the [001] crystallographic direction, we display corresponding transmission spectra of a (001) slab this the crystal, consisting of 16 layers of spheres, for LCP and RCP normally incident light (the differences between LCP and RCP components in the dispersion and transmission diagrams are not discernible in the scale of this figure). We note again that, in the case considered here, there is a distinct characterization of the bands of propagating modes as purely LCP and RCP, according to the relevant irreducible representations, E_1 and E_2, respectively, of the associated point symmetry group (C_4) [28] and thus there is no polarization conversion from LCP to RCP and vice versa. In other words, the 2×2 complex transmission matrix in the basis of circularly polarized waves, $\mathbf{t}_c$, is a diagonal matrix. The corresponding matrix in the basis of s- and p-linearly polarized waves employed in the layer-multiple-scattering method, $\mathbf{t}_l$, is given by a similarity transformation [29]:

$$\mathbf{t}_l = \mathbf{A}\mathbf{t}_c\mathbf{A}^{-1}, \quad \mathbf{A} = \frac{1}{\sqrt{2}}\begin{pmatrix} 1 & 1 \\ i & -i \end{pmatrix}. \tag{2}$$

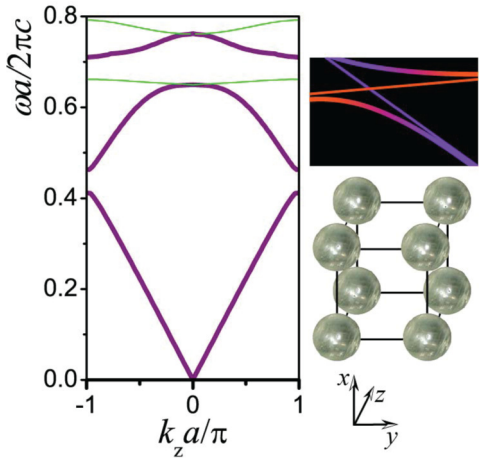

FIG. 2. (Color online) The photonic band structure of a simple-cubic crystal of unmagnetized garnet spheres, with radius to lattice constant ratio $S/a = 0.3$, in air, along its [001] direction. Thick and thin lines denote doubly degenerate and nondegenerate bands, respectively. In the margin, together with the unit cell of the crystal, we show schematically the hybridization between extended and narrow bands in the region of the magnetic-dipole resonant modes of the individual spheres.

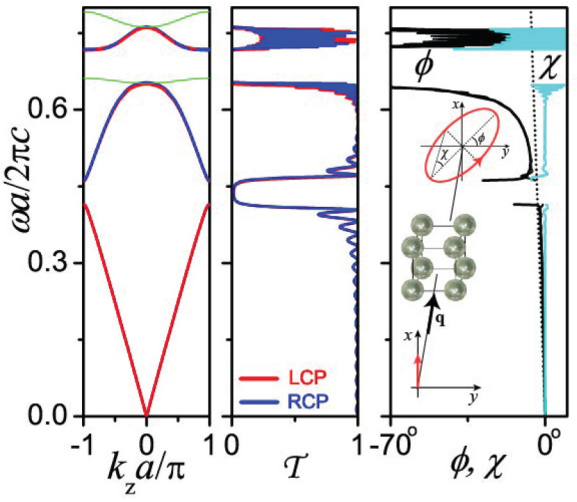

FIG. 3. (Color online) The photonic band structure of a simple-cubic crystal of magnetic garnet spheres, with radius to lattice constant ratio $S/a = 0.3$, in air, along its [001] direction, which coincides with the magnetization direction (left-hand diagram). Corresponding transmission spectra of a (001) slab of the crystal, consisting of 16 layers of spheres, for LCP and RCP normally incident light (middle diagram). The differences between LCP and RCP components in the dispersion and transmission diagrams are not discernible in the scale of the figure. Associated ellipticity and Faraday rotation angles of the wave transmitted through the above slab for x-polarized light incident in the [001] direction, as shown in the inset. By the dotted line we show the corresponding Faraday rotation angle in a homogeneous magnetic garnet slab of the same volume as the total volume of the magnetic garnet spheres in the given crystal slab (right-hand diagram).

This implies that there is polarization conversion from s to p and vice versa, which is determined by the nondiagonal elements of $\mathbf{t}_l$ that are proportional to the difference between the diagonal elements of $\mathbf{t}_c$.

A linearly polarized EM wave of angular frequency ω within the optically active bands, incident normally on the slab, is decomposed into an LCP and an RCP wave, that propagate through the slab with different phase velocities: ω/k_z^{L} and ω/k_z^{R}, respectively, where $k_z^{\mathrm{R}} - k_z^{\mathrm{L}} \equiv \Delta k_z$ is the band splitting at the given frequency. If the LCP and RCP components of the transmitted wave have the same amplitude, the transmitted wave is linearly polarized with a polarization direction at an angle

$$\phi = \tfrac{1}{2}\Delta k_z D \tag{3}$$

relative to the polarization direction of the incident wave, where D is the thickness of the slab ($16a$ in the case we consider here) and a positive ϕ means an anticlockwise rotation. In general, the transmitted wave is elliptically polarized with the long axis of the ellipse forming an angle

$$\phi = \tfrac{1}{2}\left[\arg\left(E_{\mathrm{tr}}^{\mathrm{R}}\right) - \arg\left(E_{\mathrm{tr}}^{\mathrm{L}}\right)\right] \tag{4}$$

with the polarization direction of the incident wave and with ellipticity angle

$$\chi = \arctan\frac{\left|E_{\mathrm{tr}}^{\mathrm{R}}\right| - \left|E_{\mathrm{tr}}^{\mathrm{L}}\right|}{\left|E_{\mathrm{tr}}^{\mathrm{R}}\right| + \left|E_{\mathrm{tr}}^{\mathrm{L}}\right|}, \tag{5}$$

where $E_{\mathrm{tr}}^{\mathrm{R}}$, $E_{\mathrm{tr}}^{\mathrm{L}}$ are the complex electric field amplitudes of the RCP and LCP components of the transmitted wave.

As can be seen in the right-hand diagram of Fig. 3, the ellipticity angle oscillates around zero. We note that a linearly polarized transmitted wave is obtained if $\chi = 0$. In the same diagram we also display the spectral variation of the Faraday rotation angle, ϕ, as calculated from both equations (3) and (4). The results obtained by the two equations are in good overall agreement, with the curve obtained by Eq. (4) oscillating around the smooth function $\phi(\omega)$ deduced from Eq. (3). As a general rule, the Faraday rotation increases abruptly as we approach a band gap and becomes much larger than that in a corresponding homogeneous magnetic garnet slab of the same volume as the total volume of the magnetic garnet spheres in the given crystal slab. This has also been noted and explained by others, e.g., in relation to one-dimensional magnetophotonic crystals consisting of an alternate sequence of magnetic and nonmagnetic homogeneous layers [2,3]. However, in our case, the interesting result is that the band splitting, Δk_z, and the consequent Faraday rotation, are greatly enhanced in flat band regions that correspond to modes which stem from particle resonances and are strongly localized in the spheres, namely the flat regions of the bands below the second gap, about $\omega a/2\pi c \approx 0.65$ near the Brillouin zone center, and above this gap, about $\omega a/2\pi c \approx 0.72$ near the Brillouin zone boundary.

In Fig. 4, we display an enlarged view of Fig. 3 in the latter case, where the effects are somewhat more pronounced. The Faraday rotation is defined in frequency regions where both LCP and RCP bands coexist. In Fig. 4, it can be seen that in this case the transmittance associated with each polarization exhibits strong Fabry-Perot oscillations, which stem from

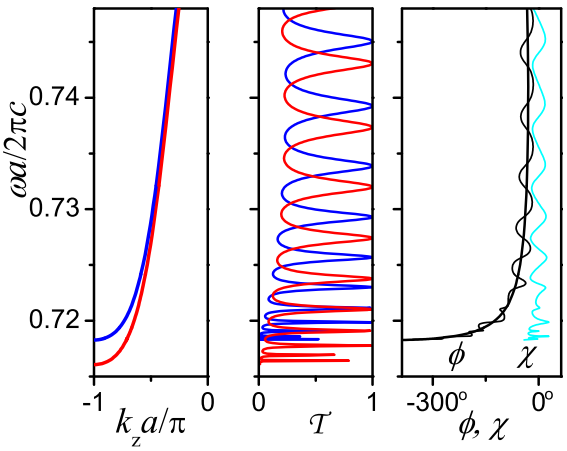

FIG. 4. (Color online) An enlarged view of Fig. 3 above the second band gap. The Faraday rotation angle ϕ is calculated by Eq. (3) (smooth curve) and Eq. (4) (oscillating curve).

miltiple reflections at the surfaces of the slab. The enhanced Faraday rotation should be understood not by a decrease of the transmission but rather by a large band splitting on the basis of Eq. (3). Indeed, the strong band splitting near the band minimum results in a clear Faraday rotation as large as $\sim -300^\circ$ for the given slab thickness, which is about 50 times larger than that in the corresponding reference homogeneous magnetic garnet slab. The Faraday rotation induced by this reference slab can be simply evaluated from Eq. (3) as follows. In a homogeneous gyrotropic medium described by a relative magnetic permeability μ_g (=1) and permittivity tensor given by Eq. (1), along the z direction, the eigenmodes of the EM field are RCP and LCP propagating plane waves with wave numbers $k_z^{\mathrm{R}} = \sqrt{\mu_g\epsilon(1-g)}\omega/c$ and $k_z^{\mathrm{L}} = \sqrt{\mu_g\epsilon(1+g)}\omega/c$, respectively. Thus to a first-order approximation Eq. (3) gives $\phi \approx -\frac{1}{2}\sqrt{\mu_g\epsilon}\,g D\omega/c$. For a (001) slab of the crystal consisting of 16 layers of spheres, the thickness of the homogeneous reference slab will be $D = 16af$, where $f = \frac{4}{3}\pi(S/a)^3$ is the volume fraction occupied by the spheres in the given crystal ($S/a = 0.3$), which yields $\phi = -8.143\omega a/2\pi c$ (in deg). Therefore, in the spectral region $\omega a/2\pi c$ from 0 to 0.8 that we consider here, the Faraday rotation induced by the reference slab varies linearly from 0° to -6.5°.

It should be noted that, though in inverse opal structures infiltrated with nickel nanoparticles a significant intrinsic (nonmagnetic) optical activity has been observed even at normal incidence [4], in the structure we study here the intrinsic geometrical rotation, induced by the crystal if the garnet spheres are unmagnetized, vanishes identically along the [001] direction, for symmetry reasons, and remains vanishingly small along an arbitrary direction. In the latter case, the polarization rotation cannot be explained in a simple manner on the basis of Eq. (3) because the bands have not a specific circular polarization character. However, in this case, we also obtain considerable magnetic optical activity in the Faraday geometry, i.e., if light propagates along the magnetization direction.

The effect of absorption can also be taken into account by adding an imaginary part to the permittivity of the particles. Considering $\epsilon = 6.25 + i0.001$, which is a reasonable value

for magnetic garnets, does not affect appreciably our results. Similar results are also expected for sparse structures of other magnetic particles in a low-refractive-index host medium, provided that they have a large permittivity and not too high losses in order to support strong localized resonances.

Finally, it is worth noting that dense particle packing does not favor strong enhancement of Faraday rotation by the mechanism we describe here, i.e., wave propagation through bands of resonant modes, because of the weaker field localization in the particles as a result of the stronger interaction of the resonant modes.

IV. CONCLUSION

In summary, by means of rigorous full electrodynamic calculations using the layer multiple scattering method, we studied the optical response of a generic three-dimensional magnetophotonic crystal, which induces a giant Faraday rotation within specific frequency ranges that can be tuned by properly choosing the geometric and material parameters involved. The proposed design consists of a sparse lattice of spherical particles made of a low-loss and high-permittivity magnetic garnet material, which support pronounced Mie resonances. The underlying mechanism traces to light propagation through collective modes that originate from these Mie resonances and are strongly localized in the magneto-optically active material thus being more efficient than band-edge states near a Bragg gap.

ACKNOWLEDGMENT

Aristi Christofi is supported by a SPIE Optics and Photonics Education Scholarship.

[1] M. Inoue, K. Arai, T. Fujii, and M. Abe, J. Appl. Phys. **85**, 5768 (1999).
[2] A. A. Fedyanin, O. A. Aktsipetrov, D. Kobayashi, K. Nishimura, H. Uchida, and M. Inoue, IEEE Trans. Magn. **40**, 2850 (2004).
[3] A. B. Khanikaev, A. B. Baryshev, P. B. Lim, H. Uchida, M. Inoue, A. G. Zhdanov, A. A. Fedyanin, A. I. Maydykovskiy, and O. A. Aktsipetrov, Phys. Rev. B **78**, 193102 (2008).
[4] J. M. Caicedo, O. Pascu, M. López-García, V. Canalejas, A. Blanco, C. López, J. Fontcuberta, A. Roig, and G. Herrantz, ACS Nano **5**, 2957 (2011).
[5] H. Marinchio, R. Carminati, A. García-Martín, and J. J. Sáenz, New J. Phys. **16**, 015007 (2014).
[6] V. I. Safarov, V. A. Kosobukin, C. Hermann, G. Lampel, J. Peretti, and C. Marliere, Phys. Rev. Lett. **73**, 3584 (1994).
[7] C. Hermann, V. A. Kosobukin, G. Lampel, J. Peretti, V. I. Safarov, and P. Bertrand, Phys. Rev. B **64**, 235422 (2001).
[8] J. B. González-Díaz, A. García-Martín, G. Armelles, J. M. García-Martín, C. Clavero, A. Cebollada, R. A. Lukaszew, J. R. Skuza, D. P. Kumah, and R. Clarke, Phys. Rev. B **76**, 153402 (2007).
[9] C. Clavero, K. Yang, J. R. Skuza, and R. A. Lukaszew, Opt. Express **18**, 7743 (2010).
[10] C. Clavero, K. Yang, J. R. Skuza, and R. A. Lukaszew, Opt. Lett. **35**, 1557 (2010).
[11] J. B. González-Díaz, A. García-Martín, J. M. García-Martín, A. Cebollada, G. Armelles, B. Sepúlveda, Y. Alaverdyan, and M. Käll, Small **4**, 202 (2008).
[12] G. X. Du, T. Mori, M. Suzuki, S. Saito, H. Fukuda, and M. Takahashi, Appl. Phys. Lett. **96**, 081915 (2010).
[13] J. C. Banthí, D. Meneses-Rodríguez, F. García, M. U. González, A. García-Martín, A. Cebollada, and G. Armelles, Adv. Mater. **24**, OP36 (2012).
[14] P. K. Jain, Y. H. Xiao, R. Walsworth, and A. E. Cohen, Nano Lett. **9**, 1644 (2009).
[15] L. Wang, K. Yang, C. Clavero, A. J. Nelson, K. J. Carroll, E. E. Carpenter, and R. A. Lukaszew, J. Appl. Phys. **107**, 09B303 (2010).
[16] L. Wang, C. Clavero, Z. Huba, K. J. Carrol, E. E. Carpenter, D. Gu, and R. A. Lukaszew, Nano Lett. **11**, 1237 (2011).
[17] G. Armelles, A. Cebollada, and A. García-Martín, J. M. Montero-Moreno, M. Waleczek, and K. Nielsch, Langmuir **28**, 9127 (2012).
[18] G. Armelles, J. B. González-Díaz, A. García-Martín, J. M. García-Martín, A. Cebollada, M. U. González, S. Acimovic, J. Cesario, R. Quidant, and G. Badenes, Opt. Express **16**, 16104 (2008).
[19] M. Caminale, L. Anghinolfi, E. Magnano, F. Bondino, M. Canepa, L. Mattera, and F. Bisio, ACS Appl. Mater. Interfaces **5**, 1955 (2013).
[20] A. V. Baryshev, H. Uchida, and M. Inoue, J. Opt. Soc. Am. B **30**, 2371 (2013).
[21] N. Stefanou, V. Yannopapas, and A. Modinos, Comput. Phys. Commun. **113**, 49 (1998).
[22] N. Stefanou, V. Yannopapas, and A. Modinos, Comput. Phys. Commun. **132**, 189 (2000).
[23] A. Christofi and N. Stefanou, Int. J. Mod. Phys. B **28**, 1441012 (2014).
[24] S. M. Drezdzon and T. Yoshie, Opt. Express **17**, 9276 (2009).
[25] A. B. Khanikaev, S. H. Mousavi, G. Shvets, and Y. S. Kivshar, Phys. Rev. Lett. **105**, 126804 (2010).
[26] K. Fang, Z. Yu, V. Liu, and S. Fan, Opt. Lett. **36**, 4254 (2011).
[27] A. García-Etxarri, R. Gómez-Medina, L. S. Froufe-Pérez, C. López, L. Chantada, F. Scheffold, J. Aizpurua, M. Nieto-Vesperinas, and J. J. Sáenz, Opt. Express **19**, 4815 (2011).
[28] T. Inui, Y. Tanabe, and Y. Onodera, *Group Theory and its Applications in Physics* (Springer, Berlin, 1990).
[29] A. Christofi, N. Stefanou, G. Gantzounis, and N. Papanikolaou, J. Phys. Chem. C **116**, 16674 (2012).